Cell

Dual Specificity Kinase DYRK3 Couples Stress Granule Condensation/Dissolution to mTORC1 Signaling

Frank Wippich,[1,3] Bernd Bodenmiller,[1] Maria Gustafsson Trajkovska,[1] Stefanie Wanka,[1] Ruedi Aebersold,[2,3] and Lucas Pelkmans[1,*]
[1]Institute of Molecular Life Sciences
[2]Faculty of Sciences
University of Zurich, Winterthurerstrasse 190, 8057 Zurich, Switzerland
[3]Department of Biology, Institute of Molecular Systems Biology, ETH Zurich, Wolfgang-Pauli-Strasse 16, 8093 Zurich, Switzerland
*Correspondence: lucas.pelkmans@imls.uzh.ch
http://dx.doi.org/10.1016/j.cell.2013.01.033

SUMMARY

Cytosolic compartmentalization through liquid-liquid unmixing, such as the formation of RNA granules, is involved in many cellular processes and might be used to regulate signal transduction. However, specific molecular mechanisms by which liquid-liquid unmixing and signal transduction are coupled remain unknown. Here, we show that during cellular stress the dual specificity kinase DYRK3 regulates the stability of P-granule-like structures and mTORC1 signaling. DYRK3 displays a cyclic partitioning mechanism between stress granules and the cytosol via a low-complexity domain in its N terminus and its kinase activity. When DYRK3 is inactive, it prevents stress granule dissolution and the release of sequestered mTORC1. When DYRK3 is active, it allows stress granule dissolution, releasing mTORC1 for signaling and promoting its activity by directly phosphorylating the mTORC1 inhibitor PRAS40. This mechanism links cytoplasmic compartmentalization via liquid phase transitions with cellular signaling.

INTRODUCTION

The nucleus and cytosol of eukaryotic cells contain numerous nonmembrane-bound compartments that consist of many proteins involved in complex reactions, such as regulation of the actin cytoskeleton and mRNA metabolism (Brangwynne et al., 2009; Li et al., 2012). Well-known among these are different types of RNA granules, microscopically visible accumulations of messenger ribonucleo-protein (mRNP) (Anderson and Kedersha, 2009; Eulalio et al., 2007). A complex repertoire of mRNP-associated proteins determines whether mRNP complexes remain silent, become translationally active, or are degraded (Buchan and Parker, 2009). Particularly during stressful conditions such as heat, oxidative and osmotic stress, virus infection, and UV irradiation, translationally silenced mRNPs accumulate into stress granules (SGs) (Anderson and Kedersha, 2008).

Recently, it has become clear that the accumulation of RNA granules is reminiscent of concentration-dependent liquid-liquid unmixing of complexes consisting of mRNA and proteins with low complexity domains (Hyman and Simons, 2012; Kato et al., 2012; Weber and Brangwynne, 2012). Although this may be a unifying principle of compartmentalization without membranes (Brangwynne et al., 2009), many fundamental questions remain unanswered. For instance, are there specific molecular regulators of this type of compartmentalization? Is such compartmentalization utilized to control signal transduction, analogous to membrane-bound compartments? These questions become apparent during cellular stress, when cells have to coordinate SG condensation and dissolution with the control of signaling pathways that initiate mRNA translation (Buchan and Parker, 2009). Among these, the mechanistic target of rapamycin (mTOR) signaling pathway takes a prominent role (Loewith and Hall, 2011; Ma and Blenis, 2009; Sengupta et al., 2010; Zoncu et al., 2011). Interestingly, in *S. cerevisiae*, TORC1 partitions in heat-induced SGs, suggesting a coupling of SG condensation and dissolution with TORC1 signaling and indicating a physiological role of SGs in the spatiotemporal regulation of TORC1 activity during stress (Takahara and Maeda, 2012). How the regulation of SG condensation and TORC1 signaling is organized is, however, unclear.

Here, we identify the dual specificity tyrosine-phosphorylation-regulated kinase 3 (DYRK3) as a protein with the ability to condense P-granule-like speckles in the cytosol and to prevent SG dissolution via its N-terminal domain when it is in a kinase-inactive form. DYRK3 couples this to the control of mTORC1 signaling by keeping mTORC1 sequestered in SGs when inactive and by phosphorylating PRAS40, a negative regulator of mTORC1 (Sancak et al., 2007; Vander Haar et al., 2007), when active. DYRK3 dynamically regulates its own partitioning between SGs and the cytosol through its kinase activity, suggesting a cyclic partitioning mechanism that couples compartmentalization through liquid phase transition with cellular signaling.

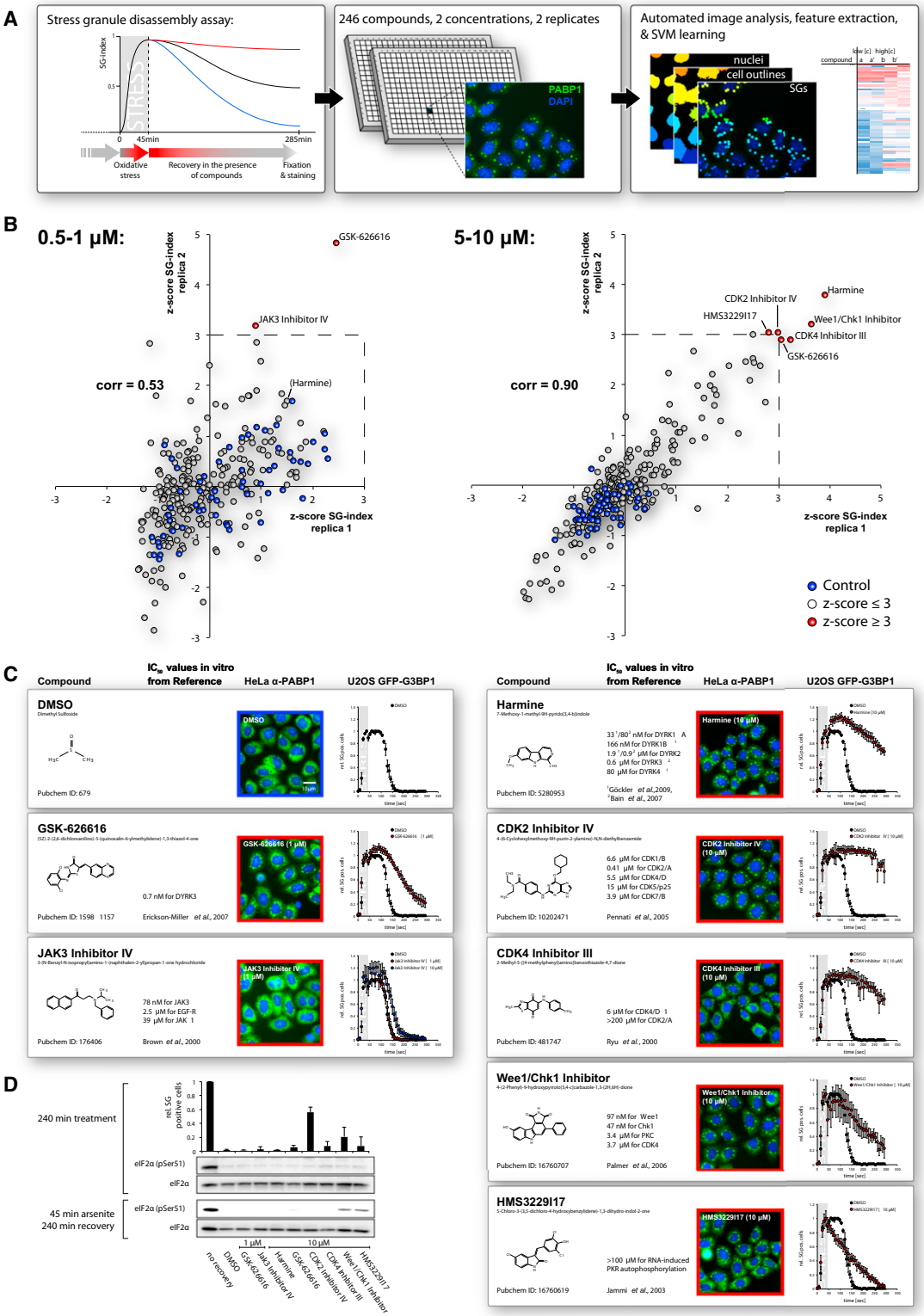

Figure 1. An Image-Based Screen for Chemical Compound Inhibitors of Stress Granule Dissolution

(A) Schematic representation of the performed image-based screen for chemical compound inhibitors. HeLa cells were exposed to oxidative stress and allowed to recover for 240 min in the presence of small compound inhibitors. The fractions of SG-positive cells were classified by immunostaining against PABP1, automated microscopy and image analysis, feature extraction, and support vector machine (SVM) learning.

(legend continued on next page)

RESULTS

An Image-Based Screen for Chemical Compound Inhibitors that Delay Stress Granule Dissolution

To study the regulation of SG dissolution, we screened a custom library of 246 small compound kinase inhibitors for their ability to prolong the presence of SGs in HeLa cells during recovery from arsenite-induced oxidative stress. We first exposed cells to arsenite for 45 min, after which we allowed recovery for 240 min in the presence of small compound inhibitors at two different concentrations (Figure 1A and Table S1 available online). To monitor the occurrence of SGs, we used immunofluorescence staining against polyadenylate-binding protein 1 (PABP1), which gets recruited to SGs upon stress, resulting in bright and easily detectable granules (Kedersha et al., 1999).

Compounds that were able to block SG dissolution for at least three standard deviations above the mean of all treatments were considered as significant hits (Z score $\geq$ 3; red dots). At 1 μM concentration, GSK-626616 and Jak3 inhibitor IV were potent in blocking SG dissolution (Figure 1B, left side), whereas at 10 μM concentration, harmine, Wee1/Chk1 inhibitor, CDK4 inhibitor III, CDK2 inhibitor IV, HMS3229I17, and GSK-626616 were potent in blocking SG dissolution (Figure 1B, right side). GSK-626616 was the most potent in delaying SG dissolution at 1 μM, whereas harmine was present in the top 4% of compounds that delayed SG dissolution at low concentrations (Figure 1B, left side), and was most potent in delaying SG dissolution at 10 μM.

To validate the seven identified compounds, we performed a second stress recovery assay using time-lapse imaging of U2OS cells stably expressing GFP-tagged Ras GTPase-activating protein-binding protein 1 (G3BP1), another marker for SGs (Ohn et al., 2008). Oxidative stress for 45 min caused a rapid increase of SG-positive cells, followed by a rapid decline in the subsequent recovery phase after arsenite washout (Figure 1C and Movie S1). The time-lapse imaging confirmed that five compounds, GSK-626616, harmine, CDK2 inhibitor IV, CDK4 inhibitor III, and Wee1/Chk1 inhibitor, reduced the decline rate of the fraction of cells with G3BP1-positive SGs during recovery.

We further excluded compounds that induce SG condensation in the absence of oxidative stress. Treatment of cells for 240 min with compounds revealed that CDK2 inhibitor IV, and to a lesser extent Wee1/Chk1 inhibitor, induced SGs in the absence of stress (Figure 1D). CDK4 inhibitor III, GSK-626616, and harmine did not cause significant SG formation in HeLa cells during 240 min of treatment.

Finally, we analyzed whether the compounds have an effect on the phosphorylation of eukaryotic initiation factor 2 alpha (eIF2α) at Ser51, which is induced by arsenite treatment and causes a translational arrest and rapid appearance of SGs (Anderson and Kedersha, 2002). Interestingly, none of the compounds could trigger the phosphorylation of eIF2α to levels comparable with those induced by arsenite, but the Wee1/Chk1 inhibitor and HMS3229I17 prevented full dephosphorylation of eIF2α after recovery from oxidative stress (Figure 1D).

Of the three compounds, which were able to reduce the rate of SGs dissolution without evoking de novo SG condensation or affecting the phosphorylation state of eIF2α, two, GSK-626616 and harmine, are known inhibitors of DYRK family kinases (Erickson-Miller et al., 2007; Göckler et al., 2009). GSK-626616 has a reported IC_{50} of 0.7 nM for DYRK3, but the overall kinase specificity is unclear.

To obtain a kinome-wide view on the specificity of GSK-626616, we profiled the inhibitory effect of GSK-626616 on 451 kinases in vitro (Karaman et al., 2008). At 0.1 μM, GSK-626616 primarily inhibits DYRK family kinases (Figure S1A and Table S2 available online) with a good selectivity (S score (35) = 0.07), comparable to well-studied and highly specific kinase inhibitors (Karaman et al., 2008). At 1 μM, GSK-626616 displays some off-target effects in vitro but still has reasonable selectivity against DYRK family kinases (S score (35) = 0.12). Harmine was previously tested on 67 kinases in vitro, and also shows a specific inhibition of DYRK family kinases at 1 μM (Bain et al., 2007), in particular of DYRK1A, DYRK2, and DYRK3 (Göckler et al., 2009).

Taken together, specific inhibitors of DYRK family kinases delay the dissolution of SGs during recovery from stress in a manner that does not involve classical SG condensation pathways via eIF2α.

DYRK3 Condenses P-Granule-like Speckles and Partitions into Stress Granules

To investigate the subcellular localization of DYRKs, we transiently expressed GFP-tagged versions in HeLa cells. Consistent with a previous classification of DYRK family kinases by their subcellular localization (Aranda et al., 2011), we found that GFP-DYRK1A and GFP-DYRK1B localized to the nucleus (Figure S2A). Interestingly, GFP-DYRK3 localized predominantly on distinct speckles distributed throughout the cytoplasm of the cell (Figure 2A). This subcellular localization of GFP-DYRK3 was not seen for GFP-DYRK2 or GFP-DYRK4, the two other class 2 DYRK family members (Figure S2A).

At low levels of expression, however, GFP-DYRK3 displayed a homogeneous distribution throughout the cytoplasm and did not condense in speckles (Figure 2B). When we correlated GFP-DYRK3 condensation with its level of expression, we discovered that it occurs in every cell when a certain threshold expression level is reached (Figure 2B). Furthermore, following GFP-DYRK3 speckles by time-lapse microscopy revealed that

(B) Representation of Z-score normalized SG-indices of the small compound inhibitors at two different concentrations (see also Table S1). Controls are colored in blue, compound conditions that are at least 3 SD above the mean of all treatments were considered as significant hits (Z score $\geq$ 3; red dots).
(C) Summary of candidate compounds and representative images from the screen, PubChem ID, chemical structure, reported IC_{50} values, and results of the time-lapse SG recovery assay in U2OS cells stably expressing GFP-G3BP1 are shown. Data are represented as mean ± SD.
(D) Ability of compounds to induce SG condensation in the absence of stress and effects of compounds on eIF2α phosphorylation in the absence and recovery from stress. Quantification of the fraction of SG-positive cells relative to arsenite-treated cells (first bar graph) for each compound at indicated concentrations is shown. Data are represented as mean ± SD (n = 3).

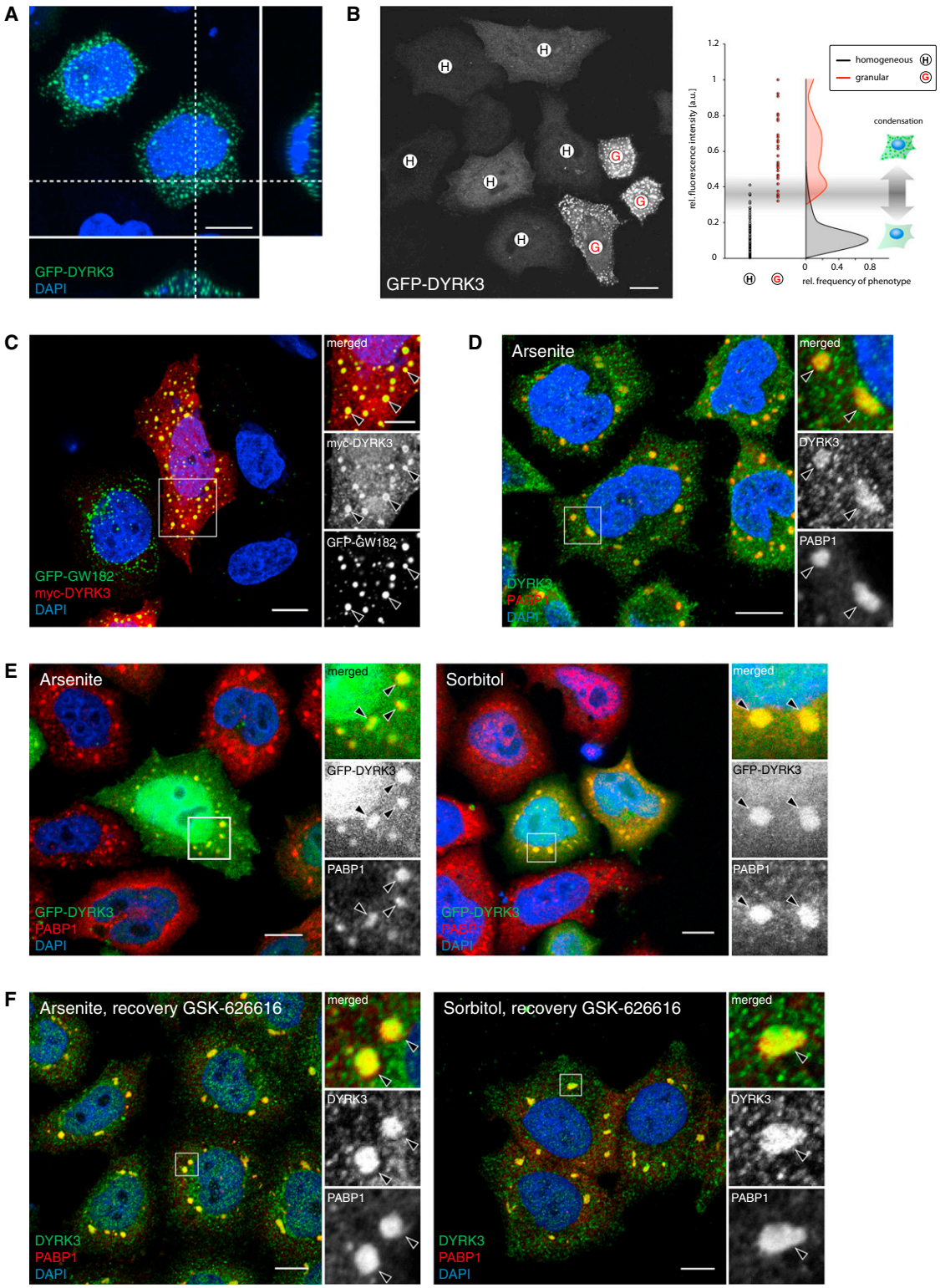

Figure 2. DYRK3 Condenses in Speckles and Partitions in Stress Granules

(A) A confocal image stack of a HeLa cell transiently expressing GFP-DYRK3 that condensed into distinct speckles distributed throughout the cytoplasm.

(B) GFP-DYRK3 condenses P-granule-like speckles in a concentration-dependent manner. A total of 241 cells were automatically segmented using computational image analysis, mean fluorescent intensity was measured per cell, and cells containing a homogeneous distribution [H] or granules [G] of GFP-DYRK3 were classified by SVM training.

(legend continued on next page)

the speckles move and merge in a liquid droplet-like manner (Figure S2B and Movie S2). These observations are reminiscent of P granule behavior in *C. elegans* (Brangwynne et al., 2009). To test whether DYRK3 condenses RNA granule components, we coexpressed myc-DYRK3 with GFP-GW182, a scaffold protein of mRNA processing bodies (P bodies) in *C. elegans*, as well as in vertebrates (Eulalio et al., 2007; Eystathioy et al., 2003). When c-expressed, myc-DYRK3 and GFP-GW182 condense in granules that were larger than formed by GFP-DYRK3 expression alone (Figure 2C).

Importantly, we observed that during oxidative and osmotic stress, endogenous DYRK3, as well as GFP-DYRK3, localizes to SGs (Figures 2D and 2E). Furthermore, DEAD box p54 protein 6 (DDX6)-positive P bodies, often in close proximity to SGs, were found docked on GFP-DYRK3-positive granules (Figure S2C). Moreover, endogenous DYRK3 remained localized to SGs after 240 min of stress recovery in the presence of DYRK inhibitors (Figures 2F and S2D).

Thus, DYRK3 has the potential to condense granules in the cytosol of human cells to which the mRNA-binding protein GW182 can be recruited, and DYRK3 localizes to SGs during oxidative and osmotic stress.

The N-Terminal Domain of DYRK3 Is Required for Stress Granule Localization and Induces Stress Granules when DYRK3 Kinase Activity Is Compromised

We next explored how inhibition of DYRK3 prevents SG dissolution. We observed that RNAi-mediated depletion of DYRK3, or of the other DYRKs (not shown), did not disturb the condensation of SGs during oxidative stress (not shown) or dissolution of SGs after oxidative stress (Figure 3A). Instead, we discovered that DYRK3 depletion, but not that of the other DYRKs (not shown), reduced the block in SG dissolution caused by GSK-626616 treatment. This suggests that inhibited DYRK3 is in a state that specifically prevents the dissolution of SGs. In support of this, we observed that expression of the kinase-deficient point mutant DYRK3-K218M is sufficient to cause the appearance of large cytoplasmic structures positive for mRNA granule markers, on which GFP-DYRK3-K218M accumulated, even in the absence of stress (Figure 3B). To test whether a specific domain of DYRK3 mediates partitioning to RNA granules, we generated a series of DYRK3 truncations (Figure 3C). Expression of DYRK3-NT, which consists of the N-terminal residues 1–188 and contains a predicted low-complexity sequence (Figure S2E) but which excludes the kinase domain and C-terminal end, induced the appearance of large granules at high expression levels (Figure 3D). Similar to SGs, these large granules had P bodies in close proximity and stained positive for PABP1 (Figure 3E). Conversely, overexpression of DYRK3 without the N-terminal domain (DYRK3-ΔNT) did not induce cytoplasmic granules and did not partition in SGs induced by oxidative stress (Figure 3F).

Thus, inhibition of DYRK3 affects SG dissolution through a specific state of DYRK3 when its kinase activity is compromised. This state depends on the N-terminal domain of DYRK3, which, when expressed alone or as part of kinase-deficient DYRK3, is able to induce the appearance of SGs in the absence of stress.

Inhibition of DYRKs Affects the Phosphorylation of Proteins that Bind mRNA, Partition in Stress Granules, and Are Downstream of mTORC1

To obtain insight into how cells couple SG condensation and dissolution to signal transduction, we next studied which signaling pathways are affected by the inhibition of DYRKs. To reveal this, we studied changes in the phosphoproteome of cells after GSK-626616 treatment, using a quantitative label-free phosphoproteomic approach (Bodenmiller et al., 2010; Huber et al., 2009) (Figure 4A). At two different time points, 30 min and 12 hr of treatment respectively, we monitored the abundance of phosphorylated peptides (Bodenmiller et al., 2007). Of the overall 1,194 peptides identified, only those peptides that were identified in three independent replicate experiments and which were significantly enriched or depleted in the GSK-626616-treated samples compared to control (DMSO) samples (t test p value: < 0.1), where taken into account (Table S3). These criteria yielded a total of 44 regulated phosphorylated peptides: 26 after short-term treatment and 18 after long-term treatment with GSK-626616, respectively (Figure 4B). Six phosphorylated peptides were found to be significantly enriched or depleted at both time points.

Eighteen out of the 22 and 7 out of the 15 corresponding proteins that were affected by short- and long-term treatment with GSK-626616, respectively, were recently reported to associate with mRNA or RNA granules (Baltz et al., 2012; Castello et al., 2012; Elvira et al., 2006; Kato et al., 2012). In addition, mTORC1 signaling regulates five of the proteins affected in each treatment (Hsu et al., 2011; Yu et al., 2011), such as the eukaryotic translation initiation factor 4E-binding protein 1 (eIF4E-BP1) at threonine 37 and 46 and the tumor suppressor protein programmed cell death 4 (PDCD4) at serine 457. Both eIF4E-BP1 and PDCD4 are translational repressors known to act downstream of the mTORC1-ribosomal protein S6 kinase 1 (S6K1) pathway (Brunn et al., 1997; Burnett et al., 1998). Similar changes in the phosphorylation of eIF4E-BP1 and PDCD4 were detected by immunoblotting using phosphorylation-specific antibodies, confirming our findings (Figure S3A). Thus, the DYRK kinase inhibitor GSK-626616 affects, among others, the phosphorylation of mRNA-associated proteins and proteins downstream of mTORC1 signaling.

(C) Transiently expressed GFP-GW182 and myc-DYRK3 display colocalization in cytoplasmic granules in unstressed cells.

(D) Endogenous DYRK3 localizes to SGs induced by oxidative stress. Cells were exposed to 0.5 mM arsenite for 45 min and immunostained for DYRK3 and PABP1.

(E) GFP-DYRK3 localizes to SGs induced by either oxidative or osmotic stress. HeLa cells expressing GFP-DYRK3 were stressed for 45 min and immune-stained for PABP1.

(F) Endogenous DYRK3 localizes to SGs induced by oxidative or osmotic stress and is retained on SGs by GSK-626616. HeLa cells were stressed for 45 min and allowed to recover in the presence of 1 μM GSK-626616 were immunostained for DYRK3 and PABP1. Scale bars, 10 μm.

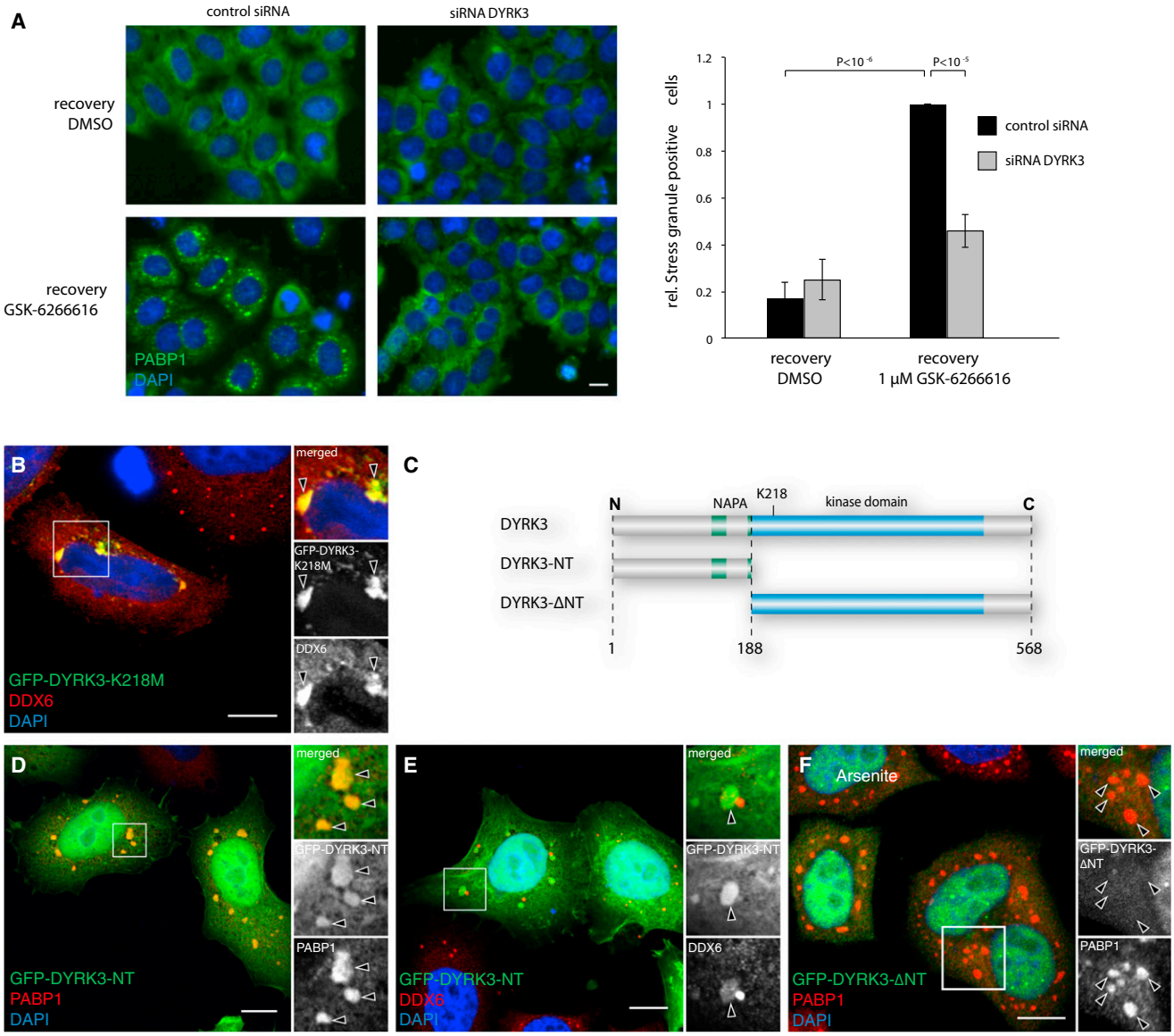

Figure 3. DYRK Kinase Activity and the N-Terminal Domain Mediate the Localization to mRNA Granules

(A) Kinase-inactive DYRK3 is responsible for the occurrence of stress granules during GSK-626616 treatment. HeLa cells were transfected with siRNA against DYRK3 for 58 hr, stressed for 45 min with 0.5 mM arsenite, and allowed to recover for 240 min in the presence or absence of 1 μM GSK-626616. Immunostaining for PABP1 allowed the identification and classification of SG-positive cells by automated image analysis and machine-learning. The fraction of SG-positive cells relative to cells transfected with control, nontargeting siRNA and treated with GSK-626616 are shown as mean ± SD (n = 3).

(B) Kinase-deficient GFP-tagged DYRK3-K218M accumulates on cytoplasmic aggregates and condenses components of mRNA granules.

(C) Schematic representation of full-length DYRK3 and different truncation mutants. Highlighted are the NAPA domains (black), the kinase domain (gray), and the ATP-binding site K218.

(D and E) The N-terminal domain of DYRK3 induces the appearance of large granules in the absence of stress. HeLa cells expressing GFP-DYRK3-NT were immunostained for PABP1 or DDX6.

(F) DYRK3 lacking the N terminus does not partition in SGs of HeLa cells stressed for 45 min. Scale bars, 10 μm.

DYRK3 Is Required for mTORC1 Activity

To validate the impact of inhibitors targeting DYRK family kinases on mTORC1 signaling, we evaluated the phosphorylation state of Thr389 of S6K1, which is considered a direct and appropriate readout for mTORC1 activity (Burnett et al., 1998). GSK-626616 treatment abolished the phosphorylation of S6K1 at Thr389 in nonstimulated HeLa cells, indicating a reduction in basal mTORC1 activity (Figure 4C). A variety of stimuli, such as epidermal growth factor (EGF) and insulin addition, can increase mTORC1 activity above basal levels (Zoncu et al., 2011). GSK-626616 treatment reduced the phosphorylation of S6K1 at Thr389 in EGF- and insulin-stimulated HeLa cells, showing that

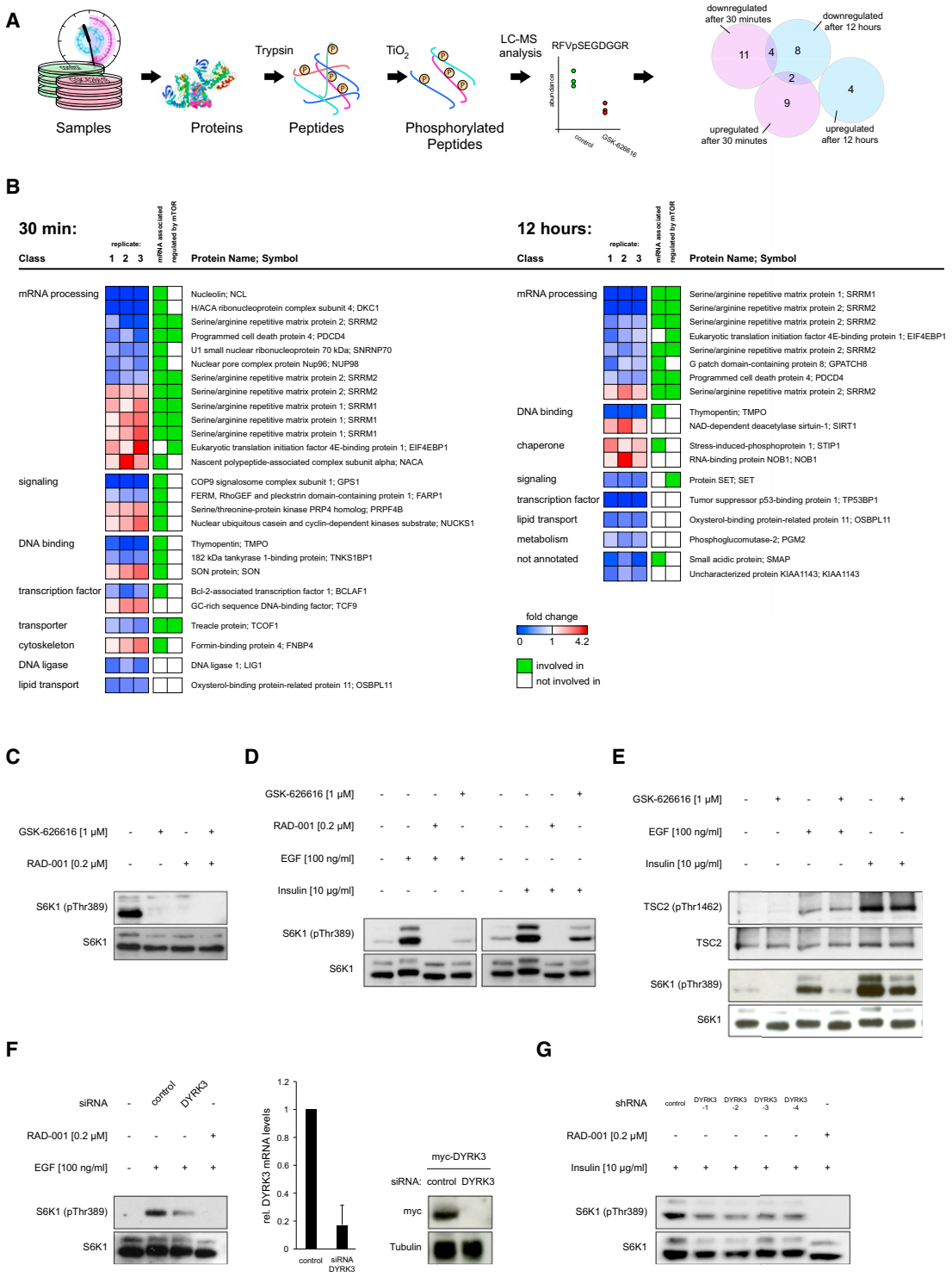

Figure 4. Quantitative Phosphoproteomic Analysis of Cells Treated with GSK-626616 Reveals Reduced mTORC1 Signaling

(A) Strategy for label-free quantitative phosphoproteomics, performed on cells treated with 0.1 μM GSK-626616 for 30 min or 12 hr, respectively. Triplicate samples were separately lysed, proteins digested, and phosphorylated peptides enriched and analyzed by mass spectrometry. A Venn diagram is shown of phosphorylated peptides found to be present in three independent replicate experiments and which abundance is significantly altered by GSK-626616.

(B) List of phosphopeptides and their single replicate fold changes in response to GSK-626616 treatment is shown for both time points. Their association with mRNA and mRNA granules (Baltz et al., 2012; Castello et al., 2012; Elvira et al., 2006; Kato et al., 2012; Voronina and Seydoux, 2010) or with mTORC1 signaling (Hsu et al., 2011; Yu et al., 2011) is highlighted in green. See Table S3.

(legend continued on next page)

mTORC1 activity is impaired (Figure 4D). The extent to which low concentrations of GSK-626616 inhibited S6K1 phosphorylation in cells was similar to the effect of a rapamycin derivative (RAD-001), a well-known inhibitor of mTORC1 (Boulay et al., 2004). Also harmine treatment was able to interfere with EGF-stimulated S6K1 phosphorylation, although to a lesser degree (Figure S3B). Moreover, GSK-626616 treatment interfered with basal mTORC1 activity, as well as EGF- or insulin-stimulated mTORC1 activity, in three additional unrelated mammalian cell lines, indicating a general mechanism that is not cell line-specific (Figure S3C). As a consequence, treatment of cells with GSK-626616 leads to a reduction in protein synthesis (Figure S3G).

The mTORC1 pathway integrates many different signaling inputs, and the DYRK kinase inhibitors may affect several of those. However, we observed no effect of GSK-626616 treatment on the phosphorylation status of tuberin (TSC2) upon stimulation of cells with either EGF or insulin (Figure 4E). In addition, we observed no effect on the phosphorylation of AKT or ERK1/2 (Figure S3D). We also found that the PI-3 kinase inhibitor Wortmannin had an additive inhibitory effect on mTORC1 activity in cells treated with GSK-626616 (Figure S3E), further indicating that the DYRK inhibitor affects mTORC1 via a parallel pathway. To assess whether the DYRK inhibitors could affect mTORC1 activity via an off-target effect, and not via inhibiting DYRKs, we considered the few in vitro off targets that these inhibitors have (Figure S3F). Two possible kinases, namely ERK8 and RSK3/4, that are weakly inhibited by GSK-626616 in vitro, might act upstream of mTORC1. However, ERK8 is not inhibited by harmine (Bain et al., 2007), and both ERK and RSK family kinases signal to mTORC1 via TSC2, whose phosphorylation status does not change during GSK-626616 treatment (Figure 4E). Finally, siRNA- and shRNA-mediated depletion of DYRK3 (but not other DYRK family kinases, data not shown) also resulted in a reduced S6K1 phosphorylation (Figures 4F and 4G). This further supports a specific effect of the inhibitors and indicates that the inhibitory effect on mTORC1 acts mainly through DYRK3 in a manner that is independent of the PI3K/AKT and ERK pathways and does not involve TSC2.

Kinase-Inactive DYRK3 Inhibits mTORC1 by Preventing Dissociation from SGs

One possibility by which inhibition of DYRK3 may result in an inhibition of mTORC1 signaling activity is by causing the sequestration of mTORC1 in SGs. In *S. cerevisiae*, dissociation from the vacuolar membrane and partitioning in SGs affects TORC1 signaling (Takahara and Maeda, 2012). Interestingly, we found that in human cells, both mTOR and the mTORC1-specific component RAPTOR are recruited to SGs induced by either osmotic or oxidative stress, and were retained on SGs by GSK-626616 treatment (Figures 5A and S4A). Furthermore, partitioning into SGs reduced the lysosomal localization of mTORC1 components (Figure S5).

While examining mTORC1 activity during and after stressful conditions, we observed a reduction in mTORC1 activity during stress, as reported previously (Inoki et al., 2003), and a hyperactivation of mTORC1 after recovery (Figure 5B). The reactivation of mTORC1 was blocked by the presence of GSK-626616 during recovery. To test whether this is a consequence of prolonged mTORC1 sequestration on SGs, we made use of the SG-dissolving property of cycloheximide (CHX), which rapidly increases the rate of SG dissolution and accelerates mTORC1 reactivation (Buchan and Parker, 2009; Takahara and Maeda, 2012). When we added CHX to cells during recovery from stress, both SG dissolution and reactivation of mTORC1 were enhanced (Figures 5B and 5C). However, addition of CHX to cells during recovery from stress in the presence of GSK-626616 led to the dissolution of SGs, but not to a full reactivation of mTORC1. We obtained similar results using emetine, which enhanced SG dissolution and mTORC1 reactivation, but, similar to CHX, led not to the reactivation of mTORC1 signaling in the presence of GSK-626616 (Figures S4D and S4E). This indicates that DYRK inhibitors reduce mTORC1 signaling by blocking SG dissolution as well as by a second mechanism, independent of mTORC1 partitioning in SGs.

DYRK3 Controls mTORC1 by Direct Phosphorylation of PRAS40

To find the second mechanism by which DYRK3 regulates mTORC1 activity independent of SG dissolution, we used a microarray for kinase substrate identification consisting of more than 9,000 different human recombinant proteins. We identified 26 candidate proteins to be directly phosphorylated in vitro by wild-type DYRK3 but not by kinase-deficient DYRK3-K218M (Figure S6A and Table S4). The second most strongly phosphorylated protein identified was the proline-rich AKT substrate of 40 kDa (PRAS40), also known as AKT1 substrate 1, which has been shown to interact directly with the mTORC1 complex and to negatively regulate mTOR kinase activity (Sancak et al., 2007; Vander Haar et al., 2007). Other proteins on the microarray that are known to regulate mTORC1 activity were not directly phosphorylated by DYRK3 (Table S4).

Phosphorylation of PRAS40 by AKT1 at Thr246 has been shown to release it from the mTORC1 complex, thereby abolishing the inhibitory effect of PRAS40 on mTOR, which allows further activation (Sancak et al., 2007; Vander Haar et al.,

(C) GSK-626616 treatment reduces basal phosphorylation of S6K1 at Thr389. Serum-deprived HeLa cells were treated for 45 min with GSK-626616 or RAD-001 and the phosphorylation status of S6K1 pThr389 was analyzed by immunoblotting of cell lysates.

(D) GSK-626616 treatment reduces EGF- and insulin-induced phosphorylation of S6K1 at Thr389. Serum-deprived HeLa cells were treated for 45 min with EGF or insulin in the absence or presence of GSK-626616 or RAD-001. See Figure S3.

(E) GSK-626616 treatment does not alter basal, EGF- or insulin-induced phosphorylation of TSC2. Serum-deprived HeLa cells were treated for 45 min with EGF or insulin in the absence or presence of GSK-626616. See Figure S3.

(F) RNAi-mediated depletion of DYRK3 reduces EGF-induced phosphorylation of S6K1 at Thr389. HeLa cells were treated for 72 hr with siRNA against DYRK3 or nontargeting siRNA, serum deprived for the last 14 hr, and treated for 45 min with EGF. Control cells were simultaneously treated with EGF and RAD-001. Knockdown efficiency was monitored by qRT-PCR and by immunoblotting of lysates of cells, transfected with myc-DYRK3. Data are represented as mean ± SD (n = 3).

(G) Depletion of DYRK3 using different shRNAs reduces insulin-induced phosphorylation of S6K1 at Thr389. Transfected, serum-deprived HeLa cells were treated 72 hr after transfection for 45 min with insulin. See Figures S3.

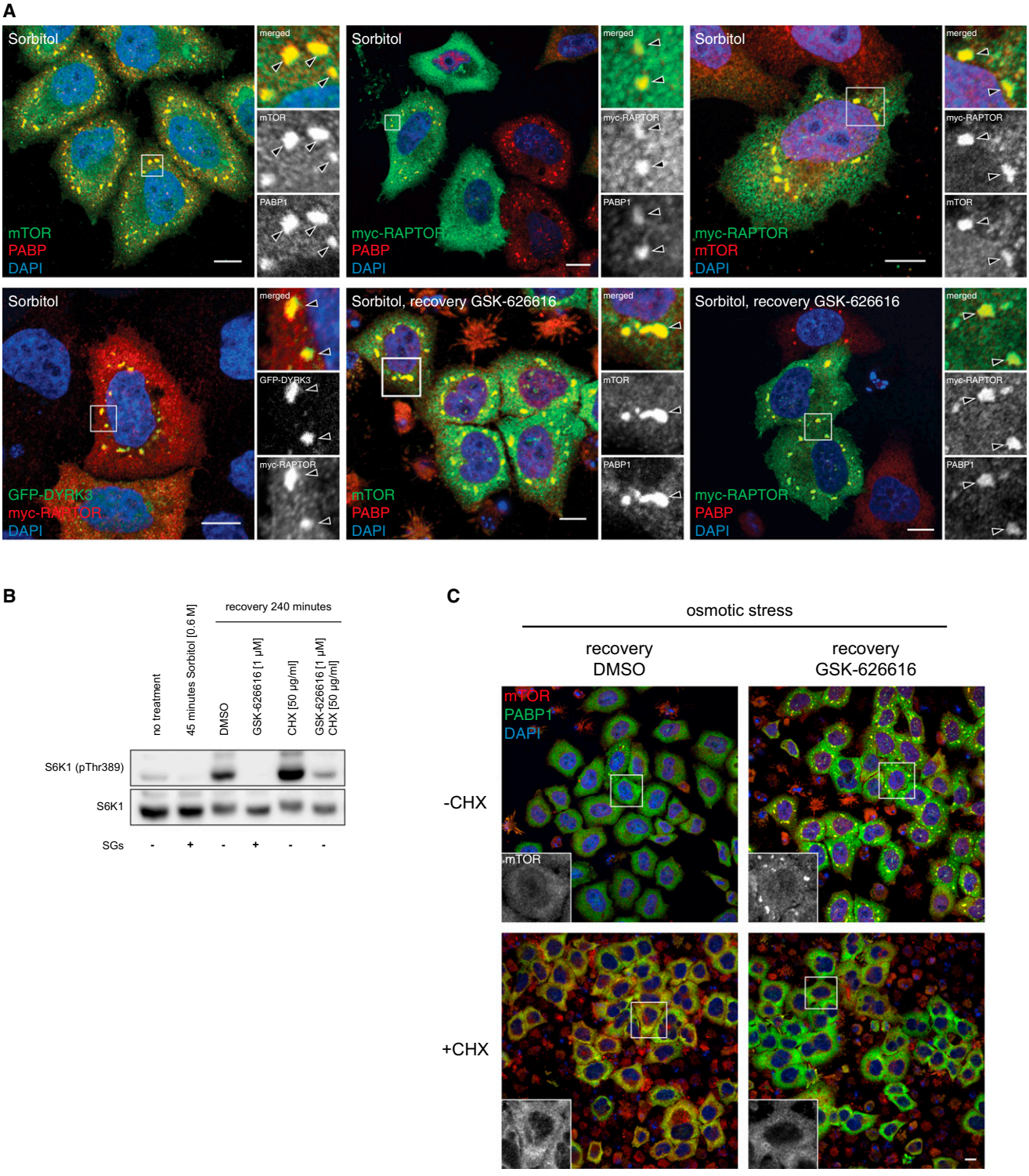

Figure 5. Osmotic Stress Leads to Partitioning of mTORC1 Components in SGs and Affects mTORC1 Signaling

(A) Components of mTORC1 localize to SGs induced by osmotic stress. Immunofluorescence of mTOR and myc-RAPTOR shows colocalization with PABP1- and GFP-DYRK3-positive SGs induced by 1 M sorbitol for 45 min. mTOR and myc-RAPTOR are retained on SGs during recovery from osmotic stress by treating cells with 1 μM GSK-626616 during 240 min recovery. See also Figure S4.

(B) Reactivation of mTORC1 activity after osmotic stress is sensitive to GSK-626616, even in the presence of CHX. The phosphorylation of S6K1 at Thr389 prior, during 45 min treatment with 0.6 M sorbitol, and after 240 min recovery in the presence of 1 μM GSK-626616, 50 μg/ml CHX, or both is shown.

(legend continued on next page)

2007). Using recombinant DYRK3 and PRAS40, we found that DYRK3 directly phosphorylates Thr246 of PRAS40 in an in vitro kinase assay (Figure 6A). Addition of GSK-626616 to this assay blocked the phosphorylation reaction in a dose-dependent manner (Figure S6B). Moreover, GSK-626616 treatment of cultured cells, as well as depletion of DYRK3, reduced the phosphorylation of PRAS40 at Thr246 in response to EGF treatment (Figures 6B and 6C).

Using coimmunoprecipitation experiments, we observed that GSK-626616 increases the fraction of bound PRAS40 to mTORC1 (Figure 6D), which is known to interfere with binding and activation of mTOR substrates (Vander Haar et al., 2007). Furthermore, expression of the T246A mutant of PRAS40, a phosphodeletion mutant able to block the stimulation of mTORC1 activity (Sancak et al., 2007), reduced S6K1 phosphorylation before stress and completely prevented mTORC1 reactivation after stress (Figure 6E).

Thus, DYRK3 directly phosphorylates PRAS40 at Thr246, a phosphorylation site responsible for regulation of PRAS40, resulting in decreased binding of PRAS40 to mTORC1, allowing activation of mTORC1 signaling in unstressed cells and reactivation of mTORC1 during stress recovery.

DYRK3 Regulates Its Own Partitioning between SGs and the Cytosol in a Cyclic Manner through Its Kinase Activity

Finally, we studied the dynamics of how DYRK3 couples SG partitioning with mTORC1 regulation. To reveal this, we performed fluorescence recovery after photobleaching (FRAP) experiments. In unstressed cells expressing GFP-DYRK3 and displaying cytoplasmic speckles, we observed that photobleached speckles quickly recovered their fluorescence signal to initial levels within 150 s (Figure 7A). Interestingly, treatment with GSK-626616 during stress recovery resulted in an entrapment of 55% of GFP-DYRK3 on granules, which did not exchange with unbleached cytosolic GFP-DYRK3. Similarly, when we photobleached the cytoplasmic aggregates induced by the kinase-deficient mutant of DYRK3 (GFP-DYRK3-K218M), we observed that 69% of the signal could not be exchanged with unbleached cytosolic signal. Thus, DYRK3 displays dynamic cycles of partitioning between SGs and the cytosol. Partitioning into SGs requires the N-terminal domain (deletion of this domain abolishes partitioning in SGs; Figure 3F), while partitioning into the cytosol requires kinase activity.

Based on these results, we propose the following mechanism by which DYRK3 couples SG condensation and dissolution with mTORC1 signaling. When SGs condense, for instance during stress, DYRK3 will partition in SGs via its N-terminal domain. Here, it contributes to preventing SG dissolution, leading to partitioning of the mTORC1 complex in SGs and thus blocking it from signaling to downstream effectors. To dissolve SGs, the kinase activity of DYRK3 is required, leading to partitioning of the mTORC1 complex in the cytosol, where DYRK3 phosphorylates PRAS40, which allows reactivation of mTORC1. Thus, DYRK3 represents a type of regulator that dynamically couples phase transition-mediated compartmentalization to signal transduction via its kinase activity.

DISCUSSION

In this study, we identify chemical compounds targeting DYRK family kinases as inhibitors of SG dissolution and show that these compounds act mainly via DYRK3. We reveal that DYRK3 has the potential to condense P-granule-like structures in the cytosol and localizes to SGs after stress. The absence of DYRK3 does not prevent SG dissolution via its N-terminal domain, but kinase-inhibited DYRK3 does. This domain is, when expressed alone or as part of a kinase-deficient mutant of DYRK3, able to induce the appearance of SG-like structures even in the absence of stress. We also show that inhibition of DYRKs affects the phosphorylation status of a number of mRNA-binding proteins and proteins downstream of mTORC1 signaling. We demonstrate that DYRK3 blocks mTORC1 signaling by keeping mTORC1 partitioned in SGs when inactive, and phosphorylates the mTORC1 inhibitor PRAS40 when active, which reduces the binding of PRAS40 to mTORC1 and allows subsequent mTORC1 activation. Furthermore, we show that mTORC1 recruitment to SGs during stress reduces its localization to lysosomes, which is required for mTORC1 activation by amino acids (Sancak et al., 2010), and explains how stress, and inhibition of DYRK3 during stress recovery, generally reduces mTORC1 activity.

The condensation of SGs via liquid-liquid unmixing depends on low complexity domains in proteins (Hyman and Simons, 2012; Kato et al., 2012; Weber and Brangwynne, 2012). The N-terminal domain of DYRK3 contains a predicted low complexity sequence, which may allow partitioning into stress granules and contribute to liquid-liquid unmixing. This is, however, not a constitutive property of the DYRK3 protein but is rather regulated by its own kinase activity in a cyclic manner.

Such a kinase-activity-dependent cycle provides an RNA-granule-sensing mechanism. When SGs condense during stress, DYRK3 senses this through its ability to cycle between SGs and the cytosol. Concomitantly, mTORC1 partitions in SGs, which prevents signaling to downstream effectors. When stress signals disappear, the kinase activity of DYRK3 will dissolve SGs by "inactivating" the SG condensation property of its N-terminal domain (and possibly by phosphorylating mRNA-binding proteins) and allowing activation of mTORC1 in the cytosol by preventing binding to PRAS40. In addition, DYRK3 might be a sensor of RNA granules that are formed under conditions different than stress, such as during cell division, cell polarization, and cell differentiation, linking their appearance to the control of mTORC1 signaling or other signal transduction pathways. We expect that further characterization of the numerous other proteins whose phosphorylation status is affected by

(C) Addition of CHX induces the dissolution of SGs and overcomes the block in SG dissolution by GSK-626616 after osmotic stress. Immunofluorescence of mTOR and PABP1 is shown in cells after 240 min recovery from 45 min 1 M sorbitol treatment. Cells were treated with 1 μM GSK-626616, 50 μg/ml CHX, or both during 240 min recovery.
Scale bars, 10 μm.

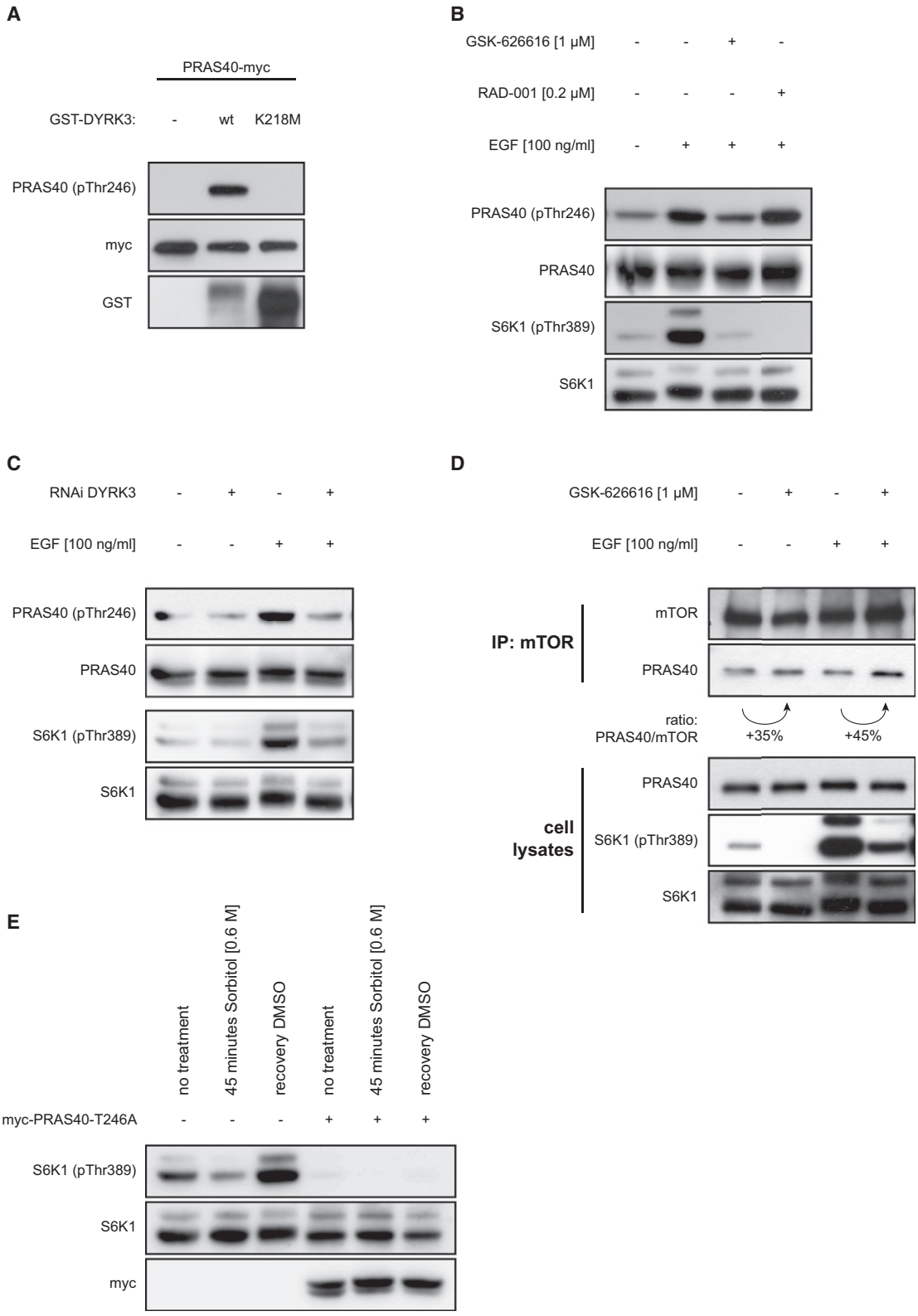

Figure 6. PRAS40 Is a Direct Substrate of DYRK3

(A) DYRK3 directly phosphorylates PRAS40 at Thr246. An in vitro kinase assay of recombinant wild-type GST-DYRK3 and kinase-deficient GST-DYRK3-K218M with recombinant PRAS40-myc was performed and phosphorylation status of Thr246 of PRAS40 was analyzed. See Figures S6.

(legend continued on next page)

inhibition of DYRKs, or which can be phosphorylated by DYRK3 in vitro, will provide further details.

Several lines of evidence suggest that the properties of DYRK3 that we have uncovered here are a conserved mechanistic principle for DYRK family members. DYRKs have been functionally linked to the cellular stress response in organisms across the eukaryotic kingdom, ranging from nutrient starvation, osmotic stress, irradiation, and genotoxic stress (Aranda et al., 2011; Moriya et al., 2001; Seifert and Clarke, 2009; Taira et al., 2007; Taminato et al., 2002; Zhang et al., 2005). Furthermore, DYRKs are constitutively active kinases, believed to be regulated by changing their subcellular localization (Aranda et al., 2011). The dynamic cycling mechanism of DYRK3 between SGs and the cytosol shares striking resemblance with that of Pom1, a DYRK kinase in *S. pombe* (Hachet et al., 2011). Pom1 cycles between a membrane-associated state, driven by autophosphorylation, and a cytosolic state, driven by phosphatase-mediated dephosphorylation of its N terminus. Our results support a similar mechanism for DYRK3. An unphosphorylated N-terminal low complexity domain might partition in SGs, whereas autophosphorylation of this domain might abolish this property, keeping it in the cytosol. This would explain how kinase-inactive DYRK3 becomes trapped in SGs, as its N-terminal domain now constitutively partitions into SGs. However, an autophosphorylation event in the N-terminal domain of DYRK3 remains to be identified, as well as a phosphatase that would dephosphorylate it.

At least two other DYRK family members have been functionally linked to mRNA granules. MBK-2, a *C. elegans* DYRK, has been observed in speckles in the cytoplasm (Stitzel et al., 2006) and is essential for the asymmetric distribution of P granules in the first cell division of the *C. elegans* embryo (Pang et al., 2004). This process depends on specifically lowering the condensation point for P granules at one site of the dividing embryo (Brangwynne et al., 2009). Analogous to the properties of DYRK3, MBK-2 might thus be involved in P granule condensation in *C. elegans*. Furthermore, mammalian DYRK1A accumulates in nuclear splicing speckles (see also Figure S2A) and is capable of dissolving speckles, depending on its kinase activity (Alvarez et al., 2003). We also observed that DYRK2, most closely related to DYRK3, localized to SGs in its inhibited state where it is partly responsible for blocking SG dissolution (data not shown).

This suggests that DYRKs are a family of kinases that couple compartmentalization through liquid phase transitions with cellular signaling through a novel kinase-dependent cyclic partitioning mechanism. Future work combining structural studies and detailed mechanistic analysis of DYRK cycling in and out of liquid-unmixed compartments with the identification of upstream factors that influence this cycle will provide further insight into how this is utilized in the regulation of various cellular processes.

EXPERIMENTAL PROCEDURES

Cell Lines and Tissue Culture

HeLa cells were from Marino Zerial (MPI-CBG, Dresden), U2OS cells (RDG3) from Paul Anderson (Brigham and Women's Hospital, Boston), and A431 cells and MEFs were from ATCC (Molsheim Cedex). All cells were maintained at 37°C under 5% CO_2 in DMEM supplemented with 10% fetal bovine serum (FBS) and Glutamax. Prior to treatments, cells were washed and serum deprived for 14 hr.

Stress Granule Condensation and Dissolution Assay

Cells were grown in 384-well plates (for initial screen, Greiner) or 8-well Lab-Tek chambers (for life cell imaging, VWR) in DMEM containing 10% FBS. Serum-deprived cells were treated for 45 min with 0.5 mM arsenite, washed twice with DMEM, and allowed to recover for 240 min in DMEM supplemented with compound inhibitors at indicated concentrations. Treatment was stopped by addition of PFA to a final concentration of 4%. SGs were stained by immunofluorescence against PABP1 and images were acquired using on an ImageXpress Micro microscope (Molecular Devices). Life cell imaging was carried out on a VisiScope Confocal Cell Explorer equipped with a 20× 0.75NA Air CFI Plan Apo VC objective (Nikon). Automatic cell detection was performed using CellProfiler (Carpenter et al., 2006). Features describing intensities and textures were used for the classification of SG-positive cells by support vector machine learning using CellClassifier (Rämö et al., 2009).

Immunofluorescence and Confocal Microscopy

HeLa cells were grown on glass coverslips and transfected with indicated plasmids using Lipofectamine 2000 according to the manufacturer's instruction. Cells were fixed by adding PFA to a final concentration of 4% and permeabilized with 0.1% Triton X-100. Unspecific binding was reduced by incubation in 1% BSA. Cells were incubated with primary antibodies overnight, followed by incubation with labeled secondary antibody for 1 hr. Nuclei were stained using DAPI. Imaging was carried out ona Leica SP5 Mid UV-VIS equipped with a 63× 1.4-0.6NA DIC, Oil, HCX Plan-Apochromat; Zeiss LSM710 equipped with a 63× 1.4NA Oil DIC Plan-Apochromat objective. Images were processed using ImageJ (http://rsb.info.nih.gov/ij/).

Phosphoproteomics

Cells were exposed to GSK-626616 or DMSO only in DMEM without FBS for 30 min and 12 hr, respectively, washed with PBS and harvested in lysis buffer (150 mM NaCl, 10 mM Tris [pH 7.2], 10 mM EDTA, 1 mM Na_3VO_4, 200 nM Ocadaic acid, 20 nM Calyculin A, EDTA free protease inhibitor [Roche], 1 mM PMSF and 0.1% *Rapi*Gest [Waters]). Three replicas were independently collected and processed separately. The isolation of phosphorylated peptides using titanium-dioxide, mass spectrometry analysis, and quantitative analysis was performed as described previously (Huber et al., 2009). Candidate protein classes were determined using PANTHER database (www.pantherdb.org).

In Vitro Kinase Substrate Identification

ProtoArray Human Protein Microarrays (PAH052406, Invitrogen) were blocked with 1% BSA in PBS for 3 hr at 4°C. Kinase Buffer (100 mM MOPS [pH 7.2], 1% Nonidet P40, 100 mM NaCl, 10 mg/ml BSA, 5 mM $MgCl_2$, 5 mM $MnCl_2$),

(B) GSK-626616 treatment reduces EGF-induced phosphorylation of PRAS40 at Thr246. Serum-deprived HeLa cells were treated for 45 min with EGF in the absence or presence of GSK-626616 or RAD-001.

(C) RNAi of DYRK3 reduces EGF-induced phosphorylation of PRAS40 at Thr246. HeLa cells were treated for 72 hr with siRNA against DYRK3 or nontargeting siRNA, serum deprived for the last 14 hr, and treated for 45 min with EGF.

(D) Binding of PRAS40 to mTORC1 is enhanced by GSK-626616 treatment. mTOR immunoprecipitates were prepared from serum-deprived or EGF-stimulated cells in the presence or absence of GSK-626616.

(E) Expression of the mutant PRAS40-T246A reduces mTORC1 signaling. HeLa cells transfected with myc-PRAS40-T246A were serum deprived and the phosphorylation of S6K1 at Thr389 prior, during 45 min treatment with 0.6 M sorbitol, and after 240 min recovery is shown.

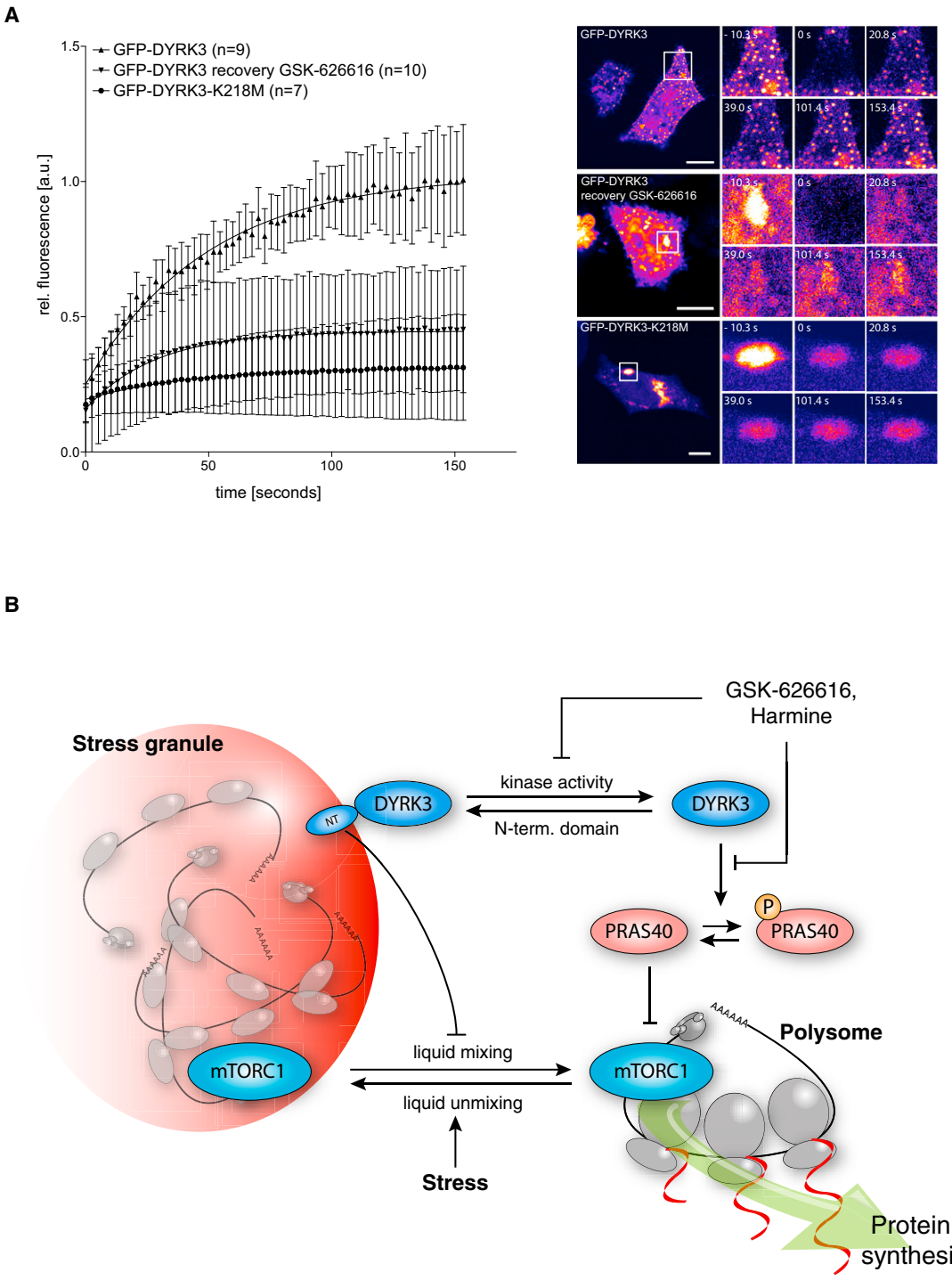

Figure 7. Activity-Dependent Dynamic Cycling of DYRK3 on SGs and Mechanism of mTORC1 Reactivation by DYRK3

(A) DYRK3 dynamically associates with mRNA granules. HeLa cells were transfected with GFP-DYRK3 or GFP-DYRK3-K218M 24 hr prior to FRAP experiments. For stress conditions (FRAP of GFP-DYRK3 on SGs after stress recovery in the presence of GSK-626616), cells were treated for 45 min with 1 M sorbitol and allowed to recover for 240 min in the presence of 1 μM GSK-626616. Data are represented as mean ± SD. A representative cell for each condition is shown as a false-color image. Scale bars, 10 μm.

(B) During stressful conditions, stress-induced translational silencing induces the condensation of SGs. DYRK3 will partition in SGs via its N-terminal domain, as well as mTORC1 components, which prevents mTORC1 signaling. When stress signals are gone, the kinase activity of DYRK3 is required for the dissolution of SGs and mTORC1 relocation to the cytosol, and for phosphorylating PRAS40, which attenuates the binding of PRAS40 to the TORC1 complex. Combined, this allows full reactivation of mTORC1 signaling.

supplemented with 33 nM γ^{33}P-ATP and 0.5 μg recombinant GST-DYRK3 or GST-DYRK3-K218M were added per array and incubated for 1 hr. Arrays were washed with 0.5% SDS, dried and exposed to Amersham Hyperfilm (GE Healthcare) for 3 hr. Analysis was carried out with ProtoArray Prospector (Invitrogen).

SUPPLEMENTAL INFORMATION

Supplemental Information includes Extended Experimental Procedures, six figures, four tables, and two movies and can be found with this article online at http://dx.doi.org/10.1016/j.cell.2013.01.033.

ACKNOWLEDGMENTS

We thank Prisca Liberali for help with the compound screen, Herbert Polzhofer for cloning GFP-DYRK3, Lilli Stergiou for help with the initial phase of this project, and all members of the Pelkmans lab for helpful discussions. We further thank Paul Anderson, Nancy Kedersha, Markku Varjosalo, and Edward Chan for reagents used in this study. F.W. is supported by a ProDoc fellowship from the Swiss National Science Foundation and is a member of the Life Science Zurich Graduate School. B.B. was supported by fellowships of the Boehringer Ingelheim Fonds and the Swiss National Science Foundation. L.P. is supported by the University of Zurich, the Swiss National Science Foundation, and the European Union. This work was supported by the SystemsX.ch RTD project PhosphoNetX.

Received: July 7, 2011
Revised: October 8, 2012
Accepted: January 10, 2013
Published: February 14, 2013

REFERENCES

Alvarez, M., Estivill, X., and de la Luna, S. (2003). DYRK1A accumulates in splicing speckles through a novel targeting signal and induces speckle disassembly. J. Cell Sci. *116*, 3099–3107.

Anderson, P., and Kedersha, N. (2002). Stressful initiations. J. Cell Sci. *115*, 3227–3234.

Anderson, P., and Kedersha, N. (2008). Stress granules: the Tao of RNA triage. Trends Biochem. Sci. *33*, 141–150.

Anderson, P., and Kedersha, N. (2009). RNA granules: post-transcriptional and epigenetic modulators of gene expression. Nat. Rev. Mol. Cell Biol. *10*, 430–436.

Aranda, S., Laguna, A., and de la Luna, S. (2011). DYRK family of protein kinases: evolutionary relationships, biochemical properties, and functional roles. FASEB J. *25*, 449–462.

Bain, J., Plater, L., Elliott, M., Shpiro, N., Hastie, C.J., McLauchlan, H., Klevernic, I., Arthur, J.S., Alessi, D.R., and Cohen, P. (2007). The selectivity of protein kinase inhibitors: a further update. Biochem. J. *408*, 297–315.

Baltz, A.G., Munschauer, M., Schwanhäusser, B., Vasile, A., Murakawa, Y., Schueler, M., Youngs, N., Penfold-Brown, D., Drew, K., Milek, M., et al. (2012). The mRNA-bound proteome and its global occupancy profile on protein-coding transcripts. Mol. Cell *46*, 674–690.

Bodenmiller, B., Mueller, L.N., Mueller, M., Domon, B., and Aebersold, R. (2007). Reproducible isolation of distinct, overlapping segments of the phosphoproteome. Nat. Methods *4*, 231–237.

Bodenmiller, B., Wanka, S., Kraft, C., Urban, J., Campbell, D., Pedrioli, P.G., Gerrits, B., Picotti, P., Lam, H., Vitek, O., et al. (2010). Phosphoproteomic analysis reveals interconnected system-wide responses to perturbations of kinases and phosphatases in yeast. Sci. Signal. *3*, rs4.

Boulay, A., Zumstein-Mecker, S., Stephan, C., Beuvink, I., Zilbermann, F., Haller, R., Tobler, S., Heusser, C., O'Reilly, T., Stolz, B., et al. (2004). Antitumor efficacy of intermittent treatment schedules with the rapamycin derivative RAD001 correlates with prolonged inactivation of ribosomal protein S6 kinase 1 in peripheral blood mononuclear cells. Cancer Res. *64*, 252–261.

Brangwynne, C.P., Eckmann, C.R., Courson, D.S., Rybarska, A., Hoege, C., Gharakhani, J., Jülicher, F., and Hyman, A.A. (2009). Germline P granules are liquid droplets that localize by controlled dissolution/condensation. Science *324*, 1729–1732.

Brunn, G.J., Hudson, C.C., Sekulić, A., Williams, J.M., Hosoi, H., Houghton, P.J., Lawrence, J.C., Jr., and Abraham, R.T. (1997). Phosphorylation of the translational repressor PHAS-I by the mammalian target of rapamycin. Science *277*, 99–101.

Buchan, J.R., and Parker, R. (2009). Eukaryotic stress granules: the ins and outs of translation. Mol. Cell *36*, 932–941.

Burnett, P.E., Barrow, R.K., Cohen, N.A., Snyder, S.H., and Sabatini, D.M. (1998). RAFT1 phosphorylation of the translational regulators p70 S6 kinase and 4E-BP1. Proc. Natl. Acad. Sci. USA *95*, 1432–1437.

Carpenter, A.E., Jones, T.R., Lamprecht, M.R., Clarke, C., Kang, I.H., Friman, O., Guertin, D.A., Chang, J.H., Lindquist, R.A., Moffat, J., et al. (2006). CellProfiler: image analysis software for identifying and quantifying cell phenotypes. Genome Biol. *7*, R100.

Castello, A., Fischer, B., Eichelbaum, K., Horos, R., Beckmann, B.M., Strein, C., Davey, N.E., Humphreys, D.T., Preiss, T., Steinmetz, L.M., et al. (2012). Insights into RNA biology from an atlas of mammalian mRNA-binding proteins. Cell *149*, 1393–1406.

Elvira, G., Wasiak, S., Blandford, V., Tong, X.K., Serrano, A., Fan, X., del Rayo Sánchez-Carbente, M., Servant, F., Bell, A.W., Boismenu, D., et al. (2006). Characterization of an RNA granule from developing brain. Mol. Cell. Proteomics *5*, 635–651.

Erickson-Miller, C.L., Creasy, C., Chadderton, A., Hopson, C.B., Valoret, E.I., Gorczyca, M., Elefante, L., Wojchowski, D.M., Chomo, M., Fitch, D.M., et al. (2007). GSK626616: A DYRK3 Inhibitor as a Potential New Therapy for the Treatment of Anemia. ASH Annual Meeting Abstracts *110*, 510.

Eulalio, A., Behm-Ansmant, I., and Izaurralde, E. (2007). P bodies: at the crossroads of post-transcriptional pathways. Nat. Rev. Mol. Cell Biol. *8*, 9–22.

Eystathioy, T., Jakymiw, A., Chan, E.K., Séraphin, B., Cougot, N., and Fritzler, M.J. (2003). The GW182 protein colocalizes with mRNA degradation associated proteins hDcp1 and hLSm4 in cytoplasmic GW bodies. RNA *9*, 1171–1173.

Göckler, N., Jofre, G., Papadopoulos, C., Soppa, U., Tejedor, F.J., and Becker, W. (2009). Harmine specifically inhibits protein kinase DYRK1A and interferes with neurite formation. FEBS J. *276*, 6324–6337.

Hachet, O., Berthelot-Grosjean, M., Kokkoris, K., Vincenzetti, V., Moosbrugger, J., and Martin, S.G. (2011). A phosphorylation cycle shapes gradients of the DYRK family kinase Pom1 at the plasma membrane. Cell *145*, 1116–1128.

Hsu, P.P., Kang, S.A., Rameseder, J., Zhang, Y., Ottina, K.A., Lim, D., Peterson, T.R., Choi, Y., Gray, N.S., Yaffe, M.B., et al. (2011). The mTOR-regulated phosphoproteome reveals a mechanism of mTORC1-mediated inhibition of growth factor signaling. Science *332*, 1317–1322.

Huber, A., Bodenmiller, B., Uotila, A., Stahl, M., Wanka, S., Gerrits, B., Aebersold, R., and Loewith, R. (2009). Characterization of the rapamycin-sensitive phosphoproteome reveals that Sch9 is a central coordinator of protein synthesis. Genes Dev. *23*, 1929–1943.

Hyman, A.A., and Simons, K. (2012). Cell biology. Beyond oil and water—phase transitions in cells. Science *337*, 1047–1049.

Inoki, K., Li, Y., Xu, T., and Guan, K.L. (2003). Rheb GTPase is a direct target of TSC2 GAP activity and regulates mTOR signaling. Genes Dev. *17*, 1829–1834.

Karaman, M.W., Herrgard, S., Treiber, D.K., Gallant, P., Atteridge, C.E., Campbell, B.T., Chan, K.W., Ciceri, P., Davis, M.I., Edeen, P.T., et al. (2008). A quantitative analysis of kinase inhibitor selectivity. Nat. Biotechnol. *26*, 127–132.

Kato, M., Han, T.W., Xie, S., Shi, K., Du, X., Wu, L.C., Mirzaei, H., Goldsmith, E.J., Longgood, J., Pei, J., et al. (2012). Cell-free formation of RNA granules: low complexity sequence domains form dynamic fibers within hydrogels. Cell *149*, 753–767.

Kedersha, N.L., Gupta, M., Li, W., Miller, I., and Anderson, P. (1999). RNA-binding proteins TIA-1 and TIAR link the phosphorylation of eIF-2 alpha to the assembly of mammalian stress granules. J. Cell Biol. *147*, 1431–1442.

Li, P., Banjade, S., Cheng, H.C., Kim, S., Chen, B., Guo, L., Llaguno, M., Hollingsworth, J.V., King, D.S., Banani, S.F., et al. (2012). Phase transitions in the assembly of multivalent signalling proteins. Nature *483*, 336–340.

Loewith, R., and Hall, M.N. (2011). Target of rapamycin (TOR) in nutrient signaling and growth control. Genetics *189*, 1177–1201.

Ma, X.M., and Blenis, J. (2009). Molecular mechanisms of mTOR-mediated translational control. Nat. Rev. Mol. Cell Biol. *10*, 307–318.

Moriya, H., Shimizu-Yoshida, Y., Omori, A., Iwashita, S., Katoh, M., and Sakai, A. (2001). Yak1p, a DYRK family kinase, translocates to the nucleus and phosphorylates yeast Pop2p in response to a glucose signal. Genes Dev. *15*, 1217–1228.

Ohn, T., Kedersha, N., Hickman, T., Tisdale, S., and Anderson, P. (2008). A functional RNAi screen links O-GlcNAc modification of ribosomal proteins to stress granule and processing body assembly. Nat. Cell Biol. *10*, 1224–1231.

Pang, K.M., Ishidate, T., Nakamura, K., Shirayama, M., Trzepacz, C., Schubert, C.M., Priess, J.R., and Mello, C.C. (2004). The minibrain kinase homolog, mbk-2, is required for spindle positioning and asymmetric cell division in early C. elegans embryos. Dev. Biol. *265*, 127–139.

Rämö, P., Sacher, R., Snijder, B., Begemann, B., and Pelkmans, L. (2009). CellClassifier: supervised learning of cellular phenotypes. Bioinformatics *25*, 3028–3030.

Sancak, Y., Thoreen, C.C., Peterson, T.R., Lindquist, R.A., Kang, S.A., Spooner, E., Carr, S.A., and Sabatini, D.M. (2007). PRAS40 is an insulin-regulated inhibitor of the mTORC1 protein kinase. Mol. Cell *25*, 903–915.

Sancak, Y., Bar-Peled, L., Zoncu, R., Markhard, A.L., Nada, S., and Sabatini, D.M. (2010). Ragulator-Rag complex targets mTORC1 to the lysosomal surface and is necessary for its activation by amino acids. Cell *141*, 290–303.

Seifert, A., and Clarke, P.R. (2009). p38alpha- and DYRK1A-dependent phosphorylation of caspase-9 at an inhibitory site in response to hyperosmotic stress. Cell. Signal. *21*, 1626–1633.

Sengupta, S., Peterson, T.R., and Sabatini, D.M. (2010). Regulation of the mTOR complex 1 pathway by nutrients, growth factors, and stress. Mol. Cell *40*, 310–322.

Stitzel, M.L., Pellettieri, J., and Seydoux, G. (2006). The C. elegans DYRK Kinase MBK-2 Marks Oocyte Proteins for Degradation in Response to Meiotic Maturation. Curr. Biol. *16*, 56–62.

Taira, N., Nihira, K., Yamaguchi, T., Miki, Y., and Yoshida, K. (2007). DYRK2 is targeted to the nucleus and controls p53 via Ser46 phosphorylation in the apoptotic response to DNA damage. Mol. Cell *25*, 725–738.

Takahara, T., and Maeda, T. (2012). Transient sequestration of TORC1 into stress granules during heat stress. Mol. Cell *47*, 242–252.

Taminato, A., Bagattini, R., Gorjão, R., Chen, G., Kuspa, A., and Souza, G.M. (2002). Role for YakA, cAMP, and protein kinase A in regulation of stress responses of Dictyostelium discoideum cells. Mol. Biol. Cell *13*, 2266–2275.

Vander Haar, E., Lee, S.I., Bandhakavi, S., Griffin, T.J., and Kim, D.H. (2007). Insulin signalling to mTOR mediated by the Akt/PKB substrate PRAS40. Nat. Cell Biol. *9*, 316–323.

Voronina, E., and Seydoux, G. (2010). The C. elegans homolog of nucleoporin Nup98 is required for the integrity and function of germline P granules. Development *137*, 1441–1450.

Weber, S.C., and Brangwynne, C.P. (2012). Getting RNA and protein in phase. Cell *149*, 1188–1191.

Yu, Y., Yoon, S.O., Poulogiannis, G., Yang, Q., Ma, X.M., Villén, J., Kubica, N., Hoffman, G.R., Cantley, L.C., Gygi, S.P., and Blenis, J. (2011). Phosphoproteomic analysis identifies Grb10 as an mTORC1 substrate that negatively regulates insulin signaling. Science *332*, 1322–1326.

Zhang, D., Li, K., Erickson-Miller, C.L., Weiss, M., and Wojchowski, D.M. (2005). DYRK gene structure and erythroid-restricted features of DYRK3 gene expression. Genomics *85*, 117–130.

Zoncu, R., Efeyan, A., and Sabatini, D.M. (2011). mTOR: from growth signal integration to cancer, diabetes and ageing. Nat. Rev. Mol. Cell Biol. *12*, 21–35.